

Numerical simulation of jet flow using LES

Petr Louda¹ Karel Kozel² Jaromír Příhoda¹

¹ Institute of Thermomechanics v.v.i., Czech Academy of Sciences, Dolejškova 5, Praha 8

² Dept. of Technical Mathematics CTU Prague, Karlovo nám. 13, CZ-121 35 Praha 2

1 Introduction

The work deals with numerical solution of plane free jet flow by large eddy simulation (LES) method. Governing system of filtered Navier-Stokes equations is completed by Smagorinsky turbulence model and instead of continuity equation Poisson equation for pressure is used. Numerical method is based on finite difference explicit scheme of second and fourth order of accuracy, using orthogonal stretched grid. Some difficulties of the simulation are discussed and first achieved results are presented.

2 Mathematical model

Basic mathematical model is the system of filtered Navier-Stokes equations for incompressible fluid

$$\frac{\partial u_j}{\partial x_j} = 0 \quad (1)$$

$$\frac{\partial u_i}{\partial t} + \frac{1}{2} \left(\frac{\partial u_j u_i}{\partial x_j} + u_j \frac{\partial u_i}{\partial x_j} + u_i \frac{\partial u_j}{\partial x_j} \right) = -\frac{\partial p}{\partial x_i} + \nu \frac{\partial^2 u_i}{\partial x_j \partial x_j} - \frac{\partial \tau_{ij}}{\partial x_j} \quad (2)$$

where $u_i = (u_1, u_2, u_3) \equiv (u, v, w)$ is vector of filtered velocity, $x_i = (x_1, x_2, x_3) \equiv (x, y, z)$ Cartesian coordinates, p filtered pressure divided by constant density of the fluid and ν is constant kinematic viscosity. The τ_{ij} is sub-grid stress tensor, which will be approximated by a turbulence model. The convective term is considered according to Arakawa as average of divergence and advective form. This conserves mean momentum as well as kinetic energy and helps to minimize aliasing errors during long time integration. The continuity equation (1) is not solved directly. Instead, a Poisson equation for pressure is obtained by computing divergence of Eq. (2)

$$\frac{\partial D}{\partial t} + \frac{1}{2} \frac{\partial}{\partial x_i} \left(\frac{\partial u_j u_i}{\partial x_j} + u_j \frac{\partial u_i}{\partial x_j} + u_i \frac{\partial u_j}{\partial x_j} \right) = -\frac{\partial^2 p}{\partial x_i^2} - \frac{\partial}{\partial x_i} \frac{\partial \tau_{ij}}{\partial x_j}, \quad D = \frac{\partial u_j}{\partial x_j} \quad (3)$$

This is the fourth equation to close the system. The first term on LHS is discretised in such a way, that continuity equation is satisfied as well.

The sub-grid turbulence is modelled by Smagorinsky eddy viscosity model in the form

$$\tau_{ij} = -2\nu_t S_{ij}, \quad S_{ij} = \frac{1}{2} \left(\frac{\partial u_i}{\partial x_j} + \frac{\partial u_j}{\partial x_i} \right) \quad (4)$$

where the eddy viscosity

$$\nu_t = (C_S \Delta)^2 \sqrt{2S_{ij}S_{ij}}, \quad (5)$$

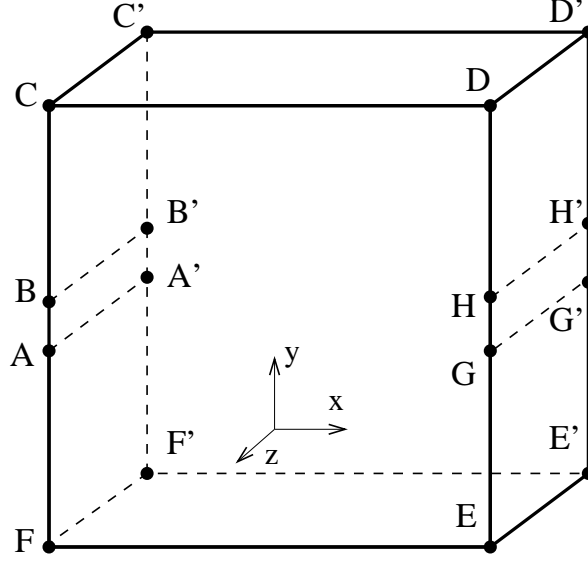


Fig. 1: Solution domain

where the Smagorinsky coefficient was chosen constant and in the range $C_S = 0.1 - 0.3$ for different simulations. The length scale Δ depends on local resolution of turbulence and on the orthogonal grid was set $\Delta = (\Delta x \Delta y \Delta z)^{1/3}$.

The plane turbulent jet is simulated in the solution domain shown in Fig. 1. The jet of initial constant (non-turbulent) velocity U_J is surrounded by a weak co-flowing stream of velocity U_c . According to the figure following boundary conditions for Eq. (2) were used

- $u = U_J, v = w = 0$ in the nozzle ABA'B'
- $u = U_c, \frac{\partial v}{\partial x} = \frac{\partial w}{\partial x} = 0$ on BCC'B' and FAA'F'
- $\frac{\partial u}{\partial y} = \frac{\partial v}{\partial y} = \frac{\partial w}{\partial y} = 0$ on upper and lower free boundaries CDD'C' and FEE'F'
- $\frac{\partial \bar{u}}{\partial x} = \frac{\partial \bar{v}}{\partial x} = \frac{\partial \bar{w}}{\partial x} = 0, \frac{\partial u'_i}{\partial t} + \bar{u} \frac{\partial u'_i}{\partial x} = 0$ on outlet boundary EDD'E'
- periodic boundary conditions on CDEF and C'D'E'F'

In the above, the velocity \bar{u}_i is filtered velocity averaged in the periodic direction and fluctuation $u'_i = u_i - \bar{u}$. The outlet boundary condition is not completely satisfactory as will be discussed below.

For pressure Poisson equation (3) the Neumann boundary condition is used on all boundaries except for periodic boundaries where periodicity condition is used.

As initial condition we set $u = U_J, v = w = 0$ in ABGHA'B'G'H' and $u = U_c, v = w = 0$ in the rest of the domain. To this velocity field random divergence-free fluctuating field is added. Maximum magnitude of the fluctuation is $0.03U_J$. The pressure is set to a constant.

3 Numerical method

The equations (2), (3) are solved by a finite difference method on a non-regular grid. All velocity components and pressure are located in same points. The momentum equations are discretized in time by second order accurate Adams-Bashforth scheme

$$\frac{U^{n+1} - U^n}{\Delta t} = \frac{3}{2}R(U^n) - \frac{1}{2}R(U^{n-1}) - \text{grad } p^{n+1} \quad (6)$$

where the unknown $U = \text{col}[u_1, u_2, u_3]$ and $R(U)$ contains all terms except for pressure gradient and time derivative. The pressure is implicit, from new time level $n+1$. By computing divergence of (6) the Poisson equation for pressure is obtained

$$\text{div}(\text{grad } p^{n+1}) = \frac{1}{\Delta t}(\text{div } U^n - \text{div } U^{n+1}) + \text{div} \left[\frac{3}{2}R(U^n) - \frac{1}{2}R(U^{n-1}) \right] \quad (7)$$

where $\text{div } U^{n+1} = 0$ is inserted and $\text{div } U^n$ is retained as a corrective term to prevent accumulation of errors in mass conservation.

The spatial discretization is done by central difference operators. The pressure gradient and sub-grid stresses are approximated by second order accurate formulas, e.g. in the x -direction

$$\left. \frac{\partial f}{\partial x} \right|_i \approx \frac{f_{i+1} - f_{i-1}}{\Delta x^+ + \Delta x^-}, \quad \left. \frac{\partial^2 f}{\partial x^2} \right|_i \approx \frac{1}{\Delta x} \left(\frac{f_{i+1} - f_i}{\Delta x^+} - \frac{f_i - f_{i-1}}{\Delta x^-} \right) \quad (8)$$

where the steps $\Delta x^+ = x_{i+1} - x_i$, $\Delta x^- = x_i - x_{i-1}$, $\overline{\Delta x} = (\Delta x^+ + \Delta x^-)/2$. For convective and viscous terms, fourth order accurate formulas according to Veldman [3] are used. The differences are obtained by Richardson extrapolation combining $8\times$ (second order accurate difference) – (second order accurate difference on a coarse grid consisting of every second grid point)

$$\left. \frac{\partial f}{\partial x} \right|_i \approx \frac{1}{2H_i}(-u_{i+2} + 8u_{i+1} - 8u_{i-1} + u_{i-2}) \quad (9)$$

$$\left. \frac{\partial^2 f}{\partial x^2} \right|_i \approx \frac{1}{H_i} \left[8 \left(\frac{f_{i+1} - f_i}{\Delta x^+} - \frac{f_i - f_{i-1}}{\Delta x^-} \right) - \left(\frac{f_{i+2} - f_i}{\Delta x^{++}} - \frac{f_i - f_{i-2}}{\Delta x^{--}} \right) \right] \quad (10)$$

where $\Delta x^{++} = x_{i+2} - x_i$, $\Delta x^{--} = x_i - x_{i-2}$, $H_i = 4(x_{i+1} - x_{i-1}) - (x_{i+2} - x_{i-2})/2$. The time step is chosen as

$$\Delta t = \min \left(\frac{CFL}{|u_i|/\Delta x_i}, \frac{C_v}{(\nu + \nu_t)/\Delta x_i^2} \right), \quad i = 1, 2, 3 \quad (11)$$

with $CFL = 0.2$, $C_v = 0.1$. The fourth order accurate differences are used as well to approximate $\text{div}(\text{grad } p)$. The Poisson equation is solved by block Gauss-Seidel method.

4 Simulations and preliminary results

The jet is determined by Reynolds number $Re = U_J|AB|/\nu$ and the velocity of the co-flow U_c . The $Re = 30\,000$ was chosen according to Hoffman [2]. The co-flow was used in [2] in order to help in overcoming specific difficulties of plane jet simulation. In the present work, the co-flow seems not critical (i.e. does not help much) and gradually was chosen very weak at $U_c = 0.01U_J$.

The plane jet simulation presents some difficulties. First, the jet always bends towards lower or upper boundary and stays in this non-physical state. This is caused by missing connection between lower and upper boundary, which would be separated by the jet. Hoffman [2] suggests that average pressure on lower and upper boundary should be equal. Therefore the pressure on upper and lower boundary is increased/decreased by half of average pressure difference. Further the correction is applied inside the domain by adding/subtracting pressure difference interpolated between value on the boundary and zero on mean jet axis. This procedure is used in the present work by modifying solution of Eq. (3) before inserting into momentum equations.

At the same stage the pressure is modified to ensure global mass conservation. If the inflow mass flux through inlet, lower and upper boundary is denoted F_{in} and the same for outlet boundary as F_{out} , then $F_{in} + F_{out} = 0$ is required. During computation the errors may accumulate and the global mass conservation would not be satisfied. Therefore an additional normal pressure gradient δp on the outlet is prescribed, which causes such an acceleration that F_{out} one time step later changes to compensate for the old imbalance:

$$\delta p = -\frac{F_{in} + F_{out}}{\Delta t S_{out}}, \quad (12)$$

where S_{out} is outlet area. This correction ensures that F_{in} and $-F_{out}$ differ typically by 0.01% only.

The Fig. 2 shows isolines of instantaneous velocity in the same z -plane after 7600 time steps from initial conditions. On the left, the outlet boundary condition is Neumann condition for all components of velocity. The large outlet velocities near axis is backward flow, which is compensated by outflow further from the axis. The inflow in time changes to outflow and back. This is computationally stable, but unphysical solution, which is basically same also in longer solution domain. The right part of the figure shows solution with combined outlet boundary condition as described in section 2. Here, the Neumann boundary condition is used for span-wise averaged velocity and fluctuations are generated by so called convective boundary condition. Although the later condition is more acceptable, large scale (non-turbulent) unsteadiness especially near outlet boundary still exists which makes averaged flow-field unsymmetrical. The convective boundary condition for the whole velocity vector, with convective velocity constant on the outlet boundary resulted in similar problems as with Neumann condition.

Next preliminary results of LES on longer grid are shown. The grid has $223 \times 283 \times 46$ nodes in x , y , z direction respectively. In the x -direction the steps increase downstream according to $\Delta x^+ / \Delta x^- = 1.0095$, smallest $\Delta x = 0.156|AB|$. The nozzle exit is divided by 8 steps, followed by 30 equal steps, then the stretching is $\Delta y^+ / \Delta y^- = 1.019$. The $\Delta z = 0.156|AB|$. The development of total kinetic energy in the solution domain (divided by number of nodes) is shown in Fig. 3. The energy very slowly increases, which may be caused by increasing entrainment of fluid on upper and lower boundary, where the flow is very slow. Other cause may be improper boundary conditions. The development of turbulence is monitored by magnitude of velocity fluctuations with respect to span-wise averaged velocity, see also Fig. 3. After the turbulence develops into a steady state the statistics data can be collected (after approx. 15 000 time steps). The steady turbulence indicates that the numerical scheme probably is not responsible for the problems with simulation. The sudden increase after 24 000 time steps seems to be related to larger scale unsteadiness, whatever caused it.

The Reynolds (ensemble) averaged statistics is obtained by averaging in time as well as in span-wise direction. Since the turbulence is approximately steady and is homogenous in span-wise (periodic) direction, by ergodic hypothesis these averaging procedures are equivalent. The Reynolds averaged flow-field is shown in Fig. 4. The Reynolds stresses are evaluated by

$$\langle u'_i u'_j \rangle = \langle u_i u_j \rangle - \langle u_i \rangle \langle u_j \rangle \quad (13)$$

where brackets denote Reynolds averaging. The resolved (i.e. without contribution of sub-grid stresses) turbulent energy $\langle u'_i u'_i \rangle / 2$ is shown in Fig. 5. The averaged velocity is unsymmetrical especially near the outlet boundary. The turbulent energy develops as expected, but large scale vortical structures influenced by the outlet boundary make it look more random further downstream.

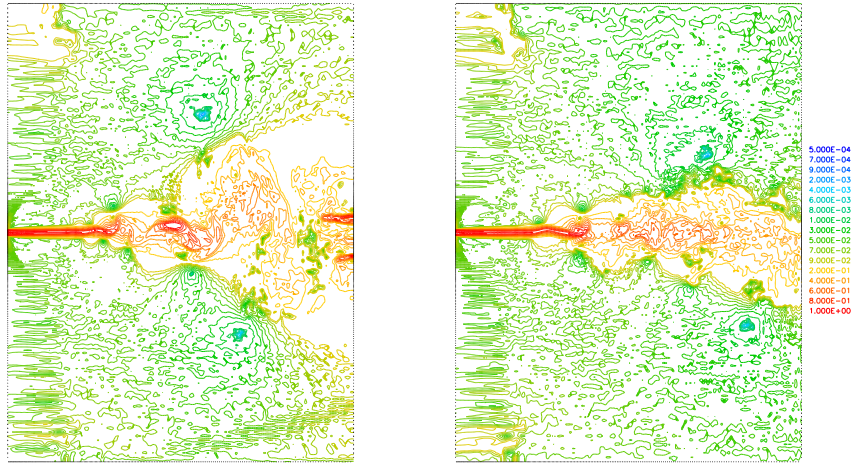


Fig. 2: Comparison of outlet boundary conditions (isolines of velocity)

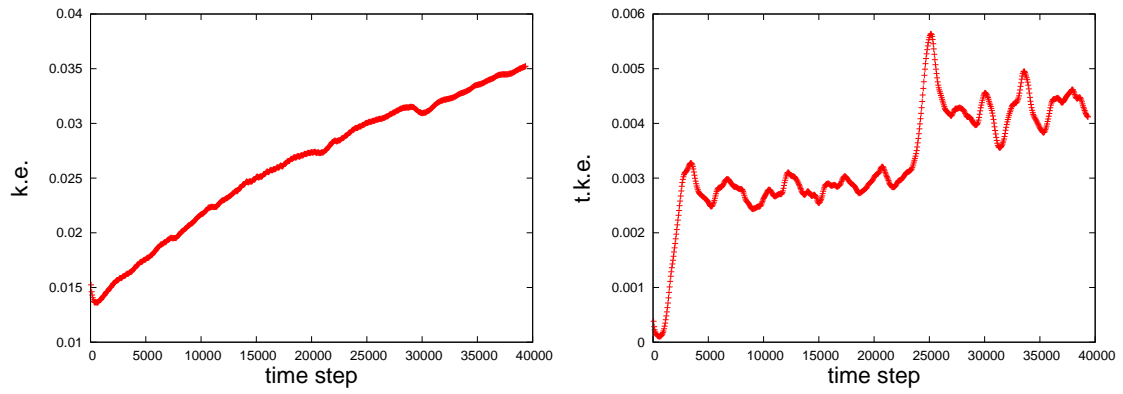


Fig. 3: Development of total kinetic energy (left) and energy of velocity fluctuations (right)

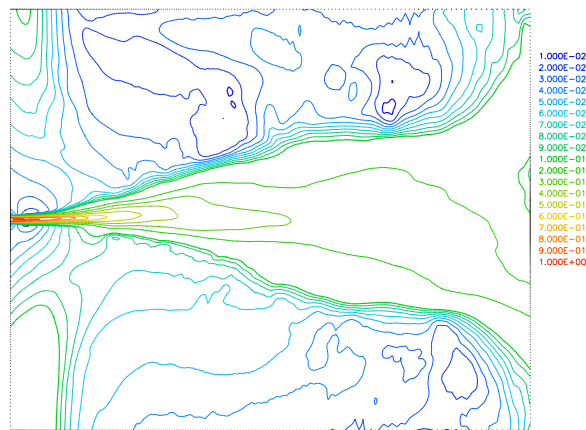


Fig. 4: Isolines of averaged velocity

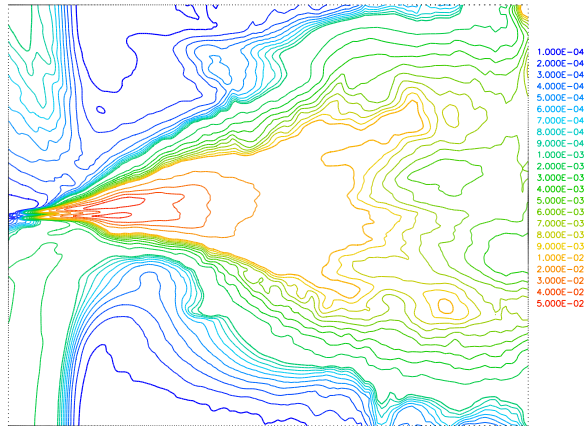


Fig. 5: Isolines of turbulent energy

5 Conclusions

The work presented a numerical method for LES of incompressible flow. The method is based on explicit scheme with fourth order accurate central approximation for convection and resolved diffusion. The pressure is obtained by solving appropriate Poisson equation. The sub-grid turbulence is modeled by Smagorinsky eddy viscosity model. Preliminary results for LES of plane turbulent jet were shown. It follows that the long time simulation is very demanding concerning boundary conditions. Further investigation of these is still necessary.

Acknowledgment

This work was partially supported by project COST OC 167, grant No. 103/09/0977 of GA CR, Research plan No. MSM 6840770010 and grant No. 201/08/0012 GA CR.

References

- [1] Arakawa, A., Computational design for long-term numerical integration of the equations of fluid motion: Two dimensional incompressible flow. Part I., J. Comp. Phys. 1 (1966) 119–143.
- [2] Hoffman, G., Engineering application of large eddy simulation to turbulent free and wall-bounded shear layers, PhD thesis, TU Muenchen 1996.
- [3] Veldman, A.E.P., Rinzema, K., Playing with nonuniform grids, J. Eng. Math. 26 (1991), 119–130.